Threshold Excitation Statistics and Imaging of Random Lasers in π-Conjugated Polymer Films; Evidence for Random Resonators

A. Tulek[#], R. C. Polson and Z. V. Vardeny*
Department of Physics & Astronomy, University of Utah, Salt Lake City, Utah 84112, USA
[#] Presently at Aselsan Inc. P.O. Box 30, Etlik 06011, Turkey

Random lasing is laser action that consists of a sequence of narrow, coherent spectral lines observed when stimulated emission in a disordered gain medium is excited above threshold excitation intensity, I_{th}. We studied three I_{th} distribution functions, $F^{(n)}(I_{th})$ in π-conjugated polymer films, where n (= 1-3) is the number of lasing random resonators in the excited film area; including their evolution with respect to the excitation area size, and polymer mixture with various concentrations of TiO_2 nanoparticles. Optical images of the excited film area support the I_{th} measurements; since the sharp laser lines in the emission spectrum are accompanied by the appearance of lasing random resonators in the picture. At I_{th}, where a single dominant random lasing resonator appears in the accompanying picture, we found good agreement between the cavity diameter extracted from the emission power Fourier transform analysis, and the cavity size in the picture. This was directly confirmed by a novel technique of space/spectrum cross-correlation of the laser emission lines with 10x10 μm^2 spatial resolution; where we show that the laser modes are indeed localized within the respective lasing resonator. We found that $F^{(1)}(I_{th})$ has both a marked asymmetry with respect to the mean threshold, $(I_{th})_{ave}$, and decreases with the area size. We also found that upon increasing the TiO_2 nanoparticles density, ρ in the polymer/TiO_2 mixture the light mean free path decreases, $F^{(1)}(I_{th})$ broadens, and $(I_{th})_{ave}$ linearly increases with ρ, indicating that the addition of extrinsic scatterers to the polymer matrix is not beneficial to random lasing. Our results provide strong evidence for the model of *random resonators* in the gain medium for explaining random lasing in π-conjugated polymer films.

*** e-mail:val@physics.utah.edu**

Random lasing (RL) is an unconventional type of laser action, in which light scattering and interference in disordered systems that contain optical gain form the necessary resonant feedback mechanism[1,2]. One way of quantifying optical gain in an active medium with disorder is that it forms sufficiently strong stimulated emission (SE) before the amplified light escapes the medium due to scattering[3]. This requirement may be formulated as:

$$\ell_s > \ell_g, \qquad (1)$$

where ℓ_s is the light mean free path, and ℓ_g is the amplification length (which is inversely proportional to the optical gain, g). Based on this definition we may distinguish between two types of disorder: (i) a 'smooth', long-range disorder having large ℓ_s, which encourages lasing because its ability to trap the SE radiation. This disorder type may be formed due to refractive index fluctuations, δn caused by long-range inhomogeneity in the gain medium. (ii) A rough, short-range disorder that is caused by strong light scatterers resulting in small ℓ_s, which is detrimental to lasing because it strongly scatters the SE radiation formed in the gain medium. In this case the optical gain needs be increased (i.e. shorter ℓ_g) in order to fulfill the inequality (1). Thus refractive index inhomogeneity in the gain medium may play a dual role for RL; the interplay between the two opposite effects of disorder in the gain medium on RL should be quite interesting.

Following the discovery of light amplification in disordered gain media with non-resonant feedback[4,5], numerous experimental[6-9] and theoretical[10-16] works have been completed for understanding its mechanism. The phenomenon was dubbed "random lasing"[17] by Lawandy and collaborators[8,18] in 1994. Soon after, Cao and co-workers and independently Frolov and co-workers observed RL with resonant feedback in ZnO[19] and π-conjugated polymer films[20], respectively. In these experiments, at intensities over the threshold excitation for lasing, I_{th} discrete emission peaks having linewidth of about 1nm were found superimposed on the amplified spontaneous emission (ASE) band[20]. Such observations are demonstrated for a π-conjugated polymer film in Fig. 1, where the RL narrow lines and their dependence on the excitation spot and excitation intensity are seen. Recently, RL has been obtained in various

disordered gain media including dye solutions with scattering nanoparticles[18,21-24], semiconductor powders[19,25,26], liquid crystals[27,28], organic-inorganic nanocomposites[29,30], organic nanofibers[31], photonic crystals[32] and π-conjugated polymers in various forms[33]. In addition, a handful of applications have been recently demonstrated such as 'laser paints'[34], random lasing in human tissues[35], and random fiber lasers[36].

Two 'schools of thought' for explaining the narrow RL lines superimposed on the ASE band have been advanced: (i) The narrow lines are caused by amplification of specific photonic states in the disordered gain medium[12,37]; this point of view was recently reviewed in Ref. 2. (ii) Random cavities exist in the gain medium, which are formed due to refraction index inhomogeneity; where the narrow emission lines are in fact laser cavity modes[13,22,33]. In this case it has been shown that power Fourier transform of the RL emission spectrum is the most convenient tool for obtaining the random cavity length of the dominant resonators in the gain medium having the highest Q-value[33,35]. Questions related with these two models are still hotly debated in the literature[38-42]. Given the present situation in the theoretical understanding of RL, novel experimental 'target' measurements are needed to clarify the ambiguity, or, in contrast accentuate the existence of several viable points of view that could explain different RL actions in the variety of disordered gain media.

Although numerous works have been performed for identifying the correct underlying mechanism of RL, research focused on the *statistical nature* of the RL threshold excitation intensity has been rather scarce[40,41]. The 'random resonator' model (model (ii) above) makes specific predictions about the statistical distribution function, $F^{(1)}(I_{th})$ of the threshold excitation intensity, I_{th} for obtaining RL[43]. This model predicts a *universal* distribution function of random resonators having decreasing probability of finding resonators with high *Q*-value in the excited area of the gain medium. This gives rise to an asymmetrical $F^{(1)}(I_{th})$ which depends on the excited area, *S*; approaching a Gaussian functional dependence for large *S*. If these predictions are found to be correct *experimentally*, then this agreement would substantially strengthen the 'random resonators' model; adding complimentary experimental evidence to the power Fourier transform analysis of RL emission spectra, which so far has been the main experimental evidence in support of this model[33,35].

In this work we chose as a disordered gain medium poly(dioctyloxy)phenyl-vinyline (DOO-PPV), a π-conjugated polymer with high photoluminescence quantum efficiency, which was synthesized in our laboratory[32] (see Methods). The polymer sample was in the form of a thin film, where the SE is trapped in the direction parallel to the surface, forming a 'wave-guiding' effect; consequently a two-dimensional (2D) disordered gain medium is a more appropriate description of this situation. The polymer film was optically pumped by the second harmonic of a pulsed Nd: YAG laser system at 532 nm, having pulse duration of ~100 ps (see Methods). We present in this work a systematic study of RL I_{th} distribution, $F^{(n)}(I_{th})$ for n = 1-3, where n is the number of cavities that appear in the picture of the film excited area (see Fig. 2).

We determined I_{th} by slowly increasing the pumping excitation intensity, I using several neutral density filters. At $I > I_{th}$ sharp laser-like lines appear in the emission spectrum superimposed on the ASE band; discrete Fourier component appear in the PFT spectrum; and simultaneously a lasing cavity image dominates the area picture (Fig. 2). As I further increases additional laser lines appear in the emission spectrum that dramatically change the PFT spectrum, and simultaneously a second lasing cavity becomes apparent in the image; this defines the 'second order' I_{th}. Similarly, a 'third order' I_{th} is defined when a third cavity appears in the picture (Fig. 2). For obtaining the distribution functions $F^{(n)}(I_{th})$ we tabulated I_{th} for the set of the first three lasing random cavities that belong to a specific excited area. This procedure was repeated for 120 non-overlapping illuminated areas on the film, obtaining three statistical histograms, $F^{(n)}(I_{th})$ (n = 1-3). We investigated $F^{(n)}(I_{th})$ as a function of the excited area size, S in pristine polymer films, and in films where the polymers are mixed with TiO_2 nanoparticles that act as light scatterers (see Methods).

Random Laser Imaging

In order to resolve the *spatial extent* from which RL is emitted we used the novel method of space/spectrum cross-correlation (SSCC) of the laser emission, based on a spectrometer equipped with a microscope objective. We imaged the emission from a circular-shaped illuminated area at I_{th} onto the entrance slit of a spectrometer, where a charge coupled device (CCD) recorded the dispersed emission with 2 μm real-space resolution in the **h**-direction of the slit long axis (see Suppl. Inf.). As a control experiment we first utilized the SSCC technique to

spatially resolve the laser emission spectrum that originates from a microdisk resonator that we fabricated on a DOO-PPV film, having a diameter $D = 47$ μm. We found (Suppl. Inf.) that most of the emission originates from the disk circumference, in agreement with whispering gallery modes in the microdisk. In addition, the lasing size extracted from the calibrated picture perfectly matched with the cavity diameter extracted from the periodicity, Δd in the PFT of the emission spectrum (Suppl. Inf.) using the relation:

$$\Delta d = nD/2. \qquad (2)$$

For the RL case with a single lasing random microcavity at I_{th} (Fig. 3), we found that unlike the microdisk, most of the RL emission originates from inside the random microcavity rather than the circumference (Figs. 3(a) and 3(b)). This can be explained as due to the 'roughness' that accompanies the random resonators formation in the disordered gain medium. In addition, there is also a marked periodicity in the emission spectrum and PFT (Figs. 3(c) and 3(d)), which confirms that a single lasing random cavity exists in the lasing area of the film. From the marked periodicity, $\Delta d = 22$ μm in the emission PFT using Eq. (2) we calculate $D \sim 25$ μm, which is in excellent agreement with $D \sim 24$ μm extracted from the calibrated CCD image (Fig. 3 (b)). This shows that the RL emission spectrum and the resonator that appears in the image picture are *correlated*. We therefore conclude that the bright spots in the excited area that appear above I_{th} (Fig. 2) are in fact responsible for the sharp lines in the RL emission spectrum; which are therefore *cavity-related laser modes*.

The existence of random resonators in the gain medium was also verified by measuring the SSCC of the laser emission lines generated at $\sim I_{th}$ with the capability of recording the emission spectrum from **10x10 micron spot** within the excited area on the film; we dub this technique detailed SSCC (DSSCC). For this purpose we designed a novel optical set up (Suppl. Inf.) in which the collected emission image on the spectrometer slit could be translated in the **x** direction perpendicular to the slit long axis, using a lens on a translation stage. For each translation stage value, X_i in the **x** direction (given in alphabetical order, from A to U) the output of the CCD camera is entrance slit height, h vs. wavelength, λ; which is divided into 20 pixels, each corresponds to 10 micron in real space. We moved the lens in the **x** direction in steps of 100

microns corresponding to 10 microns in the real space; in this way the RL emission spectrum is recorded for each 10x10 micron^2 spot of the lasing area of the sample film.

After several attempts we obtained a film lasing area where we could identify *two competing random cavities* that are close to each other and lase simultaneously, as seen in the CCD image in Fig. 4(a). At $I \sim I_{th}$ we do not expect that the lasing random resonators with the largest Q-value would be very different from each other; nevertheless, they show sufficiently different narrow lines in the emission spectrum, which makes it possible to clearly demonstrates that the lines are in fact localized within the corresponding random resonator. Within the main lasing area we measured two different well-defined periodic PFT patterns, within the two squares denoted onto the lasing area 'image'; each contains 3x3 = 9 pixels. For each '9-pixel clusters' we summed up the RL emission spectra, and also performed an average of their corresponding emission PFT (Figs. 3(b) and 3(c), respectively). A very clear periodicity related to the laser modes is seen in the emission spectrum of the left and right cavity; *although the emission spectra are quite different from each other*. The right 'cluster' emission spectrum contains a repeatable *doublet* of laser modes having separation, $\Delta\lambda \approx 1.5$ nm; whereas the left 'cluster' spectrum contains a *trio* of repeatable laser modes having approximately the same $\Delta\lambda$ as in the right 'cluster' spectrum. The corresponding PFT spectra show a prominent FT doublet component, Δd at 42 μm and 45 μm for the right and left 'cavities', respectively; and their harmonics up to d = 250 micron. Consequently using Eq. (2) and n = 1.78 we obtained $D \approx 47$ μm for the right 'cavity', and $D \approx$ 50 μm for the left 'cavity'.

We also verified that the laser modes belonging to each random resonator are indeed localized within the corresponding area of the individual microcavity. For this purpose we summed up the laser emission spectra recorded in the h-pixels of each translation stage position, X_i, and plotted the obtained spectrum as 'X_i vs. λ' (Fig. 5(b)). We note that each RL spectrum is anyhow localized in the **h** direction of the film within a group of ~ five pixels close to the center; and thus the summed spectrum at each X_i in fact represents 10 μm localization in the **x** direction within about 50 μm in the **h** direction. In this way we could follow each strong laser mode vs. X_i as depicted in Fig. 5(b). The horizontal line of the largest intensity corresponds to X_i = H, which clearly divides the figure into two 'halves'; this is the border line between the two adjacent (left

and right) 'random cavities' (Fig. 5(a)). It is clearly seen that most of the laser modes are localized within few X_i's in each respective 'half'. For example, the strongest laser mode at 630.8 nm in the lower 'half' (i.e. left cavity in Fig. 5(a)) does not show up in the upper 'half' (or right cavity); in fact it is localized within five X_i's that correspond to ~ 50 micron. Same is true for most of the laser modes in the lower 'half', such as 629.6, 629.8, 630.3 nm, etc. In contrast, most of the laser modes in the upper 'half' that corresponds to the right cavity in Fig. 5(a), do not show up in the lower 'half' (i.e. left cavity). For example, the strongest laser mode at 631.7 nm is localized within four X_i's of the upper 'half', which is ~ 40 micron localization length. The same is true for the other strong laser modes in the upper 'half', such as 627.7, and 629.5 nm. We therefore conclude that the individual laser modes *are localized within the corresponding 'cavity' area on the film, in agreement with the diameter extracted from the PFT of the laser emission spectrum*.

Excitation Threshold Distribution Functions for Random Lasing

Pristine DOO-PPV polymer film

Fig. 6(a) shows $F^{(n)}(I_{th})$ for a DOO-PPV film for n = 1-3, at a fixed excitation area size of 100 μm x 1 mm. It is seen that I_{th} range for $F^{(1)}(I_{th})$ is rather narrow, concentrated around I_{th} ~60 nJ/pulse. This implies that I_{th} for most of the RL cavities in the film having the highest Q-value *have approximately the same* I_{th}. We therefore dub these resonators as the '*dominant* cavities'[33]. The similarity among the 'dominant' random cavities in the film leads to the appearance of periodicity in the *average PFT* analysis, as discussed previously[22,33]. I_{th} for RL of higher orders is larger, and the distribution functions $F^{(n)}(I_{th})$ are broader. This indicates that the degree of inhomogeneity for RL cavities having lower Q-value in the polymer film is larger. This conclusion is also supported by the pictures taken at low and high I, above I_{th} (Suppl. Inf.).

For studying the evolution of $F^{(1)}(I_{th})$ with respect to the size, S of the illuminated area we performed the statistical measurements on the same polymer film, but at various S. Fig. 6(b) shows $F^{(1)}(I_{th})$ at increasing S; $F^{(2)}(I_{th})$ and $F^{(3)}(I_{th})$ for higher RL orders exhibited similar trends with S as that of $F^{(1)}(I_{th})$[45]. Surprisingly, I_{th} at the average intensity, $(I_{th})_{ave}$ of the distribution is smaller for the smallest S; and thus occurs at lower optical gain. This is *in contrast* with the theoretical model for light amplification of photonic modes that predicts[48] $I_{th} \sim S^{-3/4}$; and also

contradicts the recently measured I_{th} area dependence in thick films of dye/TiO_2 mixture in PMMA[46]. Both models predict that $(I_{th})_{ave}$ decreases with S; but this is not supported by the data that shows $(I_{th})_{ave}$ increases with S. This strongly indicates that RL in thin polymer films behave *very differently* from thick films containing disorder gain media, probably due to the wave-guiding effects in the former. For explaining this unusual result, we note that the likelihood of exciting a dominant cavity with the highest Q-value increases with S[43], since more random cavities are covered by the excitation area; thus $(I_{th})_{ave}$ should decrease at large S. However, at large S there are also more 'dominant cavities' that may compete with each other for the same overall optical gain, and this may increase $(I_{th})_{ave}$.

To gain further insight into the statistics of the random resonators in the polymer film, we fitted the obtained $F^{(1)}(I_{th})$ histograms using a theoretical model which was developed by Apalkov and Raikh for the 'dominant cavities' having the highest Q-value[43]. In this model the threshold distribution function, $F(I_{th})$ in a finite illuminated area is given by the relation:

$$F(I_{th}) = \frac{\beta}{I_{th}}\left(\frac{I_{th}}{I_t}\right)^{\beta} \exp\left[-\left(\frac{I_{th}}{I_t}\right)^{\beta}\right] \qquad (3)$$

where β is a dimensionless parameter that is inversely proportional to the disorder in the gain medium, and I_t is the average I_{th} in the distribution function. The line through the $F^{(1)}(I_{th})$ histograms at various S is a fit using Eq.(3) with parameters given in Table I; the good agreement obtained between the experimental results and the model supports the existence of random cavities in the gain medium. We note that $F^{(1)}(I_{th})$ becomes more symmetric as S increases; this is represented by the rise in the parameter β in Eq. (3). This behavior was actually predicted by the theory[43], and this further supports the theoretical model used here.

Films of DOO-PPV/TiO_2 mixtures

For studying the change in the distribution functions $F^{(n)}(I_{th})$ with respect to the optical scattering in the film, we performed I_{th} statistical measurements of polymer films that contain TiO_2 scatterers at various concentrations, ρ using a fixed illumination area of 100 μm x 1 mm. Figures 7(a) and 7(b) summarize the light mean free path, ℓ_s of the various concentration mixtures as determined from the CBS cone, showing that our case corresponds to the weak scattering

regime[22]. Figures 7(c) and 7(d) show the evolution of $F^{(1)}(I_{th})$ as ρ increases. It is seen that $F^{(1)}(I_{th})$ is broader at larger ρ having smaller ℓ_s; this indicates increasing disorder in the film. This conclusion is supported by the pictures taken at I_{th} (Suppl. Inf.). In addition, the distribution center at $(I_{th})_{ave}$ increases with ρ, showing a linear dependence (Fig. 7(d)). The substantial increase of $(I_{th})_{ave}$ with ρ is due to the increased light scattering in the gain medium, as indicated by the decrease in ℓ_s (Fig. 7(b)). The TiO_2 balls efficiently scatter the SE radiation outside the RL resonators, and this *lowers* the random resonator *Q*-value. We therefore conclude that the main effect of adding light scatterers to the polymer chains is *decreasing* ℓ_s; and consequently increasing $(I_{th})_{ave}$.

These properties are also captured by the theoretical model that we used above. The lines through the $F^{(1)}(I_{th})$ histograms in Fig. 7(c) are based on a fit using Eq. (3) with parameters given in Table I. The good agreement obtained between the theoretical model and $F^{(1)}(I_{th})$ histograms shows that the different excitation areas on the film are *statistically independent* from each other, and therefore the disorder medium is, on average homogeneous containing no fluctuations *larger* than the sample area[43]. Here the parameter β can be directly related to the mean free path ℓ_s [43], because both values decrease with increasing disorder in the gain medium. We note, however that the parameter β decreases more slowly with ρ than ℓ_s (Table I); in fact we found empirically that $\beta \sim (\ell_s)^{1/2}$. This sub-linear empirical relation may be caused because we measured ℓ_s using 3D-like bulk samples, whereas RL occurs in a quasi-2D film configuration.

We understand the effect of light scatterers on RL in π-conjugated polymer thin films within a more general model that deals with the influence of disorder on light properties[49]. We conjecture two kinds of disorder in the polymer/TiO_2 film: (i) A smooth disorder that originates from fluctuations, δn in the effective refraction index caused by inhomogeneity in the deposited *pristine film* such as distribution of film thickness, rough surfaces, and higher density polymer inclusions caused by insufficient solubility[13]. This type of long-range disorder actually *encourages* RL because it tends to trap light in random resonators having refraction index n + δn, higher than the average refraction index, n of the polymer film[33]. However this disorder type cannot be quantified by the CBS technique that we measured on thick films. (ii) A second type of

disorder is associated with the strong TiO_2 scatterers in the mixtures that influence the light mean free path, ℓ_s, as determined by the CBS cone in the bulk; where increasing ρ in the mixture decreases ℓ_s (Fig. 7(b)). This type of disorder is detrimental to RL, and is responsible for the higher $(I_{th})_{ave}$ at larger ρ (Fig. 7(d)).

Summary: In summary, we studied three RL distribution function orders of I_{th}, $F^{(n)}(I_{th})$ in a π-conjugated polymer film of DOO-PPV, as a function of excitation area and TiO_2 scatterers concentration; the measurements were supported by image pictures of the film lasing area taken at the same excitation intensity. The obtained $F^{(n)}(I_{th})$ show that RL in polymer films originates from random cavities, each that lases above a threshold excitation intensity. This conclusion was supported by the image pictures, PFT of the emission spectrum, and space/spectrum cross-correlation function of the RL modes. We showed that at I_{th} there is a one-to-one correspondence between the size of the random resonators obtained from the image and SSCC spectrum, and the power PFT analysis of the emission spectrum; and that the RL emission spectrum originates from the localized random cavity in the excited area. We found that $F^{(1)}(I_{th})$ is asymmetric for small illumination areas, but becomes symmetric and narrower for large areas; in agreement with a previous model that predicted the existence of 'typical dominant cavity' in the film having high Q-value and lasing probability[43]. When TiO_2 scatterers are introduced into the polymer film, $F^{(1)}(I_{th})$ shows that larger and more dispersed random laser cavities having lower Q-value are formed. This is attributed to the decrease in the light mean free path in the gain medium at increased TiO_2 balls density. We conclude that *extrinsic scattering is detrimental* to random lasing, in contrast to the 'light amplification of photonic states' model for random lasing[37]. Our results may accentuate the debate on the underlying mechanism of RL in disordered media[2], by bringing *strong evidence* for an alternative model, namely that of lasing random resonators in the active medium above threshold that may be described by pre-localized photonic states[44]; this model is viable *at least* for excited π-conjugated polymer films.

Methods

Polymer films: We used poly(dioctyloxy)phenyl-vinyline (DOO-PPV), a π-conjugated polymer having high photoluminescence quantum efficiency, which was synthesized in our laboratory. The polymer powder was dissolved in toluene with a concentration of 10 mg/ml, and

subsequently casted onto a glass substrate using a spinner at 1000 RPM that formed a uniform film with a thickness of ~2 μm. Since the polymer refraction index, n = 1.78 at 630 nm is larger than that of the substrate and air, respectively; these films form *wave-guides* for the resulting SE radiation above I_{th}. Following the film formation, a 'post annealing' process was performed at 80^0 C for 6 hours under rough vacuum condition, in order to dry out the solvent used for the polymer solution. Nevertheless these films were visibly inhomogeneous, containing chunks of undisolved polymer powder, and also non-uniform thickness; these defects may be the seed of refraction index inhomogeneity in the film that is responsible for the 'smooth disorder' mentioned in the text.

Polymer and TiO_2 scatterers: For investigating the influence of scatterers in the gain medium on the RL excitation threshold, TiO_2 dielectric balls having an average diameter of 200 ± 5 nm were introduced to the DOO-PPV solution with various concentrations, as quantified by the weight ratio between the mixture constituents; and subsequently solid films were casted from the solutions. The TiO_2 balls were chosen as light scatterers because of their large refraction index (n = 2.7) that leads to a large contrast with the polymer refraction index (= 1.78). This enhances the balls scattering cross section, σ_s estimated[46] to be about 10^{-15} m^2. For calibration purpose we note that weight concentration, ρ = 10% roughly corresponds to ball density N = $5x10^{19}$ m^{-3}. We measured the light mean free path, ℓ_s of these mixtures using the coherent backscattering (CBS) technique with He:Ne laser beam at 633 nm in a *bulk sample form*. This technique gave reliable ℓ_s in mixtures with weight concentration, ρ > 5%; whereas the CBS cone was very weak for the pristine π-conjugated polymers in a 3D bulk geometry that is necessary for obtaining CBS.

The optical excitation and collection set up: The polymer films were optically pumped by the second harmonic of a pulsed Nd:YAG laser system operating at 532 nm, having pulse duration of ~100 ps at 870 Hz repetition rate. The sample films were kept under dynamic vacuum of 10^{-3} Torr for preventing photo-oxidization that is known to occur in films of π-conjugated polymers at ambient conditions. A shutter was used in the laser excitation system for minimizing the film exposure time to the laser light during the 'idle time', when measurements were not performed. The excited area on the films was in the form of a stripe having a width of 100 micrometers,

which was formed using a cylindrical lens; an iris with variable size was utilized to vary the excited stripe length and consequently the exposed area, S on the film, *without changing the excitation intensity*. Light emission from the polymer film was collected along the stripe direction using a glass fiber of 1 mm diameter, which was connected to a charge-coupled-device (CCD) attached to a spectrometer system having spectral resolution of about 0.1 nm. A computer interface connected to the CCD array was employed to record and analyze the emission spectrum from the excited film (see Fig. 1(c) inset); and a fast Fourier transform algorithm was performed on the RL emission spectra for obtaining the power Fourier transform (PFT) spectra. For the pictures of the illuminated area we used a microscope with variable magnifications and a built in CCD array. The image from the illuminated film was focused onto the microscope entrance slit from underneath the film, away from the optical collection system.

Determination of laser excitation threshold and I_{th} distribution functions: We determined I_{th} in the polymer film by slowly increasing the pumping excitation intensity, I using several calibrated neutral density filters. A power meter was also used for measuring the laser excitation power at the beginning and end of each measurement set. As I increases above I_{th}, sharp laser-like lines appear in the emission spectrum superimposed on the broader ASE background band, and simultaneously a lasing cavity image appears in the image picture of the excited area. For obtaining the distribution functions, $F^{(n)}(I_{th})$ we tabulated I_{th} for the set of the first three lasing random cavities that appear in a specific excited area (see Fig. 2). This procedure was repeated for 120 non-overlapping illuminated areas on the film, for obtaining three statistical histograms, $F^{(n)}(I_{th})$ for the first three random cavities (i.e. n = 1-3) that appear in the obtained pictures. The histograms binning in I_{th} was chosen according to the resolution of the measurements in I, which is determined by the number of measurement steps (neutral density filters) in the intensity range where the distribution occurs. We used this procedure for measuring $F^{(n)}(I_{th})$ at excitation areas having respective dimension of 0.5 mm, 1 mm, and 2 mm x 100 μm. Similar measurements were repeated for the films containing mixtures of the polymer with TiO_2 nanoparticles, with polymer to balls weight ratios of 5:1 and 8:1, measured at a fixed excitation area of 100 μm x 1 mm.

Additional information

Supplementary Information accompanies this paper on www.nature.com. Correspondence and requests for materials should be addressed to Z. V. V.

References

1. Noginov, M. A. *Solid-State Random Lasers* (Springer Series in Optical Sciences, Vol. 105, Springer, Berlin, 2005).
2. Wiersma, D. S. The Physics and Applications of random lasers. *Nature Physics* **4**, 359-367 (2008).
3. Siegman, A. E. *Lasers* (Univ. Science Books, Mill Valley, 1986).
4. Letokhov, V. S. Generation of light by scattering medium with negative resonance Absorption. *Zh. Eksp. Teor. Fiz.* **53**, 1442-1447 (1967); *Sov. Phys. JETP* **26**, 835-840 (1968).
5. Ambartsumyan, R. V., Basov, N. G., Kryukov, P. G. & Letokhov, V. S. A laser with a nonresonant feedback. *IEEE J. Quantum Electron.* **QE-2**, 442-446 (1966).
6. Markushev, v. M., Zolin, V. F. &Briskina, Ch. M. Powder laser. *Zh. Prikl. Spektrosk.* **45**, 847-850 (1986).
7. Gouedard, C., Husson, D., Sauteret, C., Auzel, F. & Migus, A. Generation of spatially incoherent short pulses in laser-pumpoed neodymium stoichiometric crystals and powders. *J.Opt. Soc. Am. B* **10**, 2358-2362 (1993).
8. Lawandy, N. M., Balachandrian, R. M., Gomes, A. S. L. & Sauvain, E. Laser action in strongly scattering media. *Nature* **368**, 436-438 (1994).
9. Sha, W.L., Liu, C. H. & Alfano R. R. Spectral and temporal measurements of laser action of Rhodamine-640 dye in strongly scattering media. *Opt. Lett.* **19**, 1922-1924 (1994).
10. John, S. & Pang, G. Theory of lasing in a multiple-scattering medium. *Phys. Rev. A* **54**, 3642-3652 (1996).
11. Beenakker, C. W. J. Thermal radiation and amplified spontaneous emission from a random medium. *Phys. Rev. Lett.* **81**, 1829-1832 (1998).
12. Jiang, X. & Soukoulis, C. M. Time Dependent Theory for Random Lasers. *Phys. Rev. Lett.* **85**, 70-73 (2000).
13. Apalkov, V. M., Raikh, M. E. & Shapiro, B. Almost localized photon modes in continuous and discrete models of disordered media. *J. Opt. Soc. Am. B* **21**, 132-140 (2004).
14. Türeci, H. E., Ge, L., Rotter, S. & Stone, A. D. Strong Interactions in Multimode Random Lasers. *Science* **320**, 643-646 (2008).

15. Hackenbroich, G., Viviescas, C., Elattari, B. & Haake, F. Photocount Statistics of Chaotic Lasers. *Phys. Rev. Lett*. **86**, 5262-5265 (2001).
16. Zaitsev, O. Spacing statistics in two-mode random lasing. Phys. Rev. A **76**, 043842 (2007).
17. Wiersma, D. S., van Albada, M. P. & Lagendijk, A. Random lasers? *Nature* **373**, 203-204 (1995).
18. Balachandran, R. M., Pacheco, D. P. & Lawandy, N. M. Laser action in polymeric gain media containing scattering particles. *Appl. Opt.* **35**, 640-643 (1996).
19. Cao, H., Zhao, Y. G., Ho, S. T., Seelig, E. W., Wang, Q. H. & Chang, R. P. H. Random laser action in semiconductor powder. *Phys. Rev. Lett.* **82**, 2278-2281 (1999).
20. Frolov, S. V., Vardeny, Z. V., Yoshino, K., Zakhidov, A. & Baughman, R. H. Stimulated emission in high-gain organic media. *Phys. Rev. B Rapid Commun*. **59**, 5284-5287 (1999).
21. Mujumdar, S., Ricci, M., Torre, R. & Wiersma, D. S. Amplified extended modes in random lasers. *Phys. Rev. Lett.* **93**, 053903 (2004).
22. Polson, R. C. & Vardeny, Z. V. Organic random lasers in the weak scattering regime, *Phys. Rev. B* **71**, 045205 (2005).
23. Wu, X., Fang, W., Yamilov, A., Chabanov, A. A., Asatryan, A. A., Botten, L. C. & Cao, H. Random lasing in weakly scattering systems. *Phys. Rev. A* **74**, 053812 (2006).
24. Popov, O., Zilbershtein, A. & Davidov, D. Random lasing from dye-gold nanoparticles in polymer films: Enhanced gain at the surface-plasmon-resonance wavelength. *Appl. Phys. Lett.* **89**, 191116 (2006).
25. Noginov, M. A., Noginova, N. E., Caulfield, H. J., Venkateswarlu, P., Thompson, T., Mahdi, M. & Ostroumov, V. Short-pulsed stimulated emission in the powders of $NdAl_3(BO_3)_4$, $NdSc_3(BO_3)_4$, and $Nd:Sr_5(PO_4)_3F$ laser crystals. *J. Opt. Soc. Am. B* **13**, 2024-2033 (1996).
26. Noginov, M. A., Zhu, G., Frantz, A. A., Novak, J., Williams, S. N. & Fowlkes, I. Dependence of $NdSc_3(BO_3)_4$ random laser parameters on particle size. *J. Opt. Soc. Am. B* **21**, 191-200 (2004).
27. Liu, Y. J., Sun, X. W., Elim, H. I. & Ji, W. Gain narrowing and random lasing from dye-doped polymer-dispersed liquid crystals with nanoscale liquid crystal droplets. *Appl. Phys. Lett.* **89**, 011111 (2006).
28. Strangi, G., Ferjani, S., Barna, V., De Luca, A., Versace, C., Scaramuzza, N. & Bartolino,

R. Random lasing and weak localization of light in dye-doped nematic liquid crystals. *Optics Express* **14**, 7737-7744 (2006).

29. Anglos, D., Stassinopoulos, A., Das, R. N., Zacharakis, G., Psyllaki, M., Jakubiak, R., Vaia, R. A., Giannelis, E. P. & Anastasiadis, S. H. Random laser action in organic–Inorganic nanocomposites. *J. Opt. Soc. Am. B* **21**, 208-213 (2004).
30. Sun, B. Q. & Jiang, D. S. Photon localization and lasing in disordered GaN_xAs_{1-x} optical superlattices. *Phys. Rev. B* **73**, 195112 (2006).
31. Quochi, F., Cordella, F., Mura, A., Bongiovanni, G., Balzer, F. & Rubahn, H. G. Gain amplification and lasing properties of individual organic nanofibers. *Appl. Phys. Lett.* **88**, 041106 (2006).
32. Polson, R. C., Chipouline, A. & Vardeny, Z. V. Random lasing in π-conjugated films and infiltrated opals. *Adv. Mater.* **13**, 760-764 (2001).
33. Polson, R. C., Raikh, M. E. & Vardeny, Z. V. Universality in unintentional laser resonators in π-conjugated polymer films. *C. R. Physique* **3**, 509-521 (2002).
34. Lawandy, N. M. "Paint-On Lasers" Light the Way for New Technologies. *Photonics Spectra*, July 119-124 (1994).
35. Polson, R. C. & Vardeny, Z. V. Random lasing in human tissues. *Appl. Phys. Lett.* **85**, 1289-1291 (2004).
36. de Matos, C. J. S., Menezes, L. D. S., Brito-Silva, A. M., Gamez, M. A. M., Gomes, A. S. L. & De Araujo, C. B. Random fiber laser. *Phys. Rev. Lett.* **99**, 153903 (2007).
37. Cao, H., Xu, J. Y., Ling, Y., Burin, A. L., Seeling, E. W., Liu, X. & Chang, R. P. H. Random lasers with coherent feedback. *IEEE J. Quan. Elec.* **9**, 111-119 (2003).
38. Van der Molen, K. l., Tjerkstra, r. W., mosk, A. P. & Lagendijk, A. Spatial extent of random laser modes. *Phys. Rev. Lett*. **98**, 143901 (2007).
39. Vanneste, C., Sebbah, P. & Cao, H. Lasing with resonant feedback in weakly scattering random systems. *Phys. Rev. Lett.* **98**, 143902 (2007).
40. Lepri, S., Cavalieri, S., Oppo G. L. & Wiersma, D. S. Statistical regimes of random laser fluctuations. *Phys. Rev. A* **75**, 063820 (2007).
41. Wu, X. & Cao, H. Statistical studies of random-lasing modes and amplified spontaneous emission spikes in weakly scattering systems. *Phys. Rev. A* **77**, 013832 (2008).
42. Milner, V. & Genack, A. Z. Photon localization laser; low-threshold lasing in random

amplifying layered medium via wave localization. *Phys. Rev. Lett.* **94**, 073901 (2005).

43. Apalkov, V. M. & Raikh, M. E. Universal fluctuations of the random lasing threshold in a sample of a finite area. *Phys. Rev. B* **71**, 054203 (2005); Erratum, ibid **72**,189903 (2005).
44. Apalkov, V. M., Raikh, M. E. & Shapiro, B. Random resonators and pre-localized modes in disordered dielectric films. *Phys. Rev. Lett*. **89**, 016802 (2002).
45. Tulek, A. Laser action in π-conjugated semiconductors. PhD thesis, University of Utah, August 2008, unpublished.
46. X. Meng, K. Fujita, S. Murai, and K. Tanaka, *Phys. Rev. A* **79**, 053817 (2009).
47. Polson, R. C., Levina, G. & Vardeny, Z. V. Spectral Analysis of Polymer Microring Lasers. *Appl. Phys. Lett.* **76**, 3858-3860 (2000).
48. Y. Ling, H. Cao, A. L. Burin, M. A. Ratner, X. Liu, and R. P. H. Chang, *Phys. Rev. A* **64**, 063808 (2001).
49. Wiersma, D. S., Bartolini, P., Lagendijk, A. & Righini, R. Localization of light in a disordered medium. *Nature* **390**, 671-673 (1997).
50. We thank M. Raikh and B. Shapiro for many helpful discussions. The measurements were performed at the John Dixon Laser Institute. This work was supported in part by the DOE Grant No. 04-ER-46109 at the University of Utah. A. Tulek is grateful for the support of the Institute of Material Science and Nanotechnology (UNAM) at Bilkent University.

UU IR Author Manuscript

Table I

The best fitting parameters, β (inversely proportional to the disorder), and I_t (the mean intensity in $F(I_{th})$) used to fit the threshold intensity distributions shown in Figs. 6 and 7, using Eq. (3).

	β	I_t (nJ/pulse)
A=0.5 mm x 100 μm	3.8	42
A=1mm x 100 μm	6.5	63
A=2 mm x 100 μm	7.2	63
0 % (TiO_2:DOO-PPV)	7.6	64
12.5 % (TiO_2:DOO-PPV)	5.3	215
20 % (TiO2:DOO-PPV)	4.1	421

Figure Captions

Figure 1 | Properties of random laser emission spectra. **a** Emission spectra of random lasers from various excited area on a DOO-PPV film, obtained at excitation intensity I = 200 nJ/pulse on an area of 100 μm x 1 mm. The smooth horizontal lines are the 'zero intensity' of the respective emission, which are displaced respect to each other for clarity. **b** Random laser spectra from a fixed illuminated spot, but at various excitation intensities I. The spectrum at I = 33 nJ/pulse is below the laser excitation threshold, I_{th}. **c** RL emission intensity vs. I that shows threshold intensity, I_{th} = 133 nJ/pulse (vertical dash line). The inset shows schematically the measurement setup.

Figure 2 | Random laser spectra of a DOO-PPV film vs. *I* compared with the illuminated area pictures. **a** shows image pictures of the excited area, where arrows emphasize lasing random cavities. At low I only one random cavity lases; at higher I two cavities lase; while at the highest I many random cavities lase together. **b** shows the RL emission spectra; and **c** is the power Fourier transform of the spectra shown in **b**, where the obtained periodicity indicates the formation of a random cavity in the excited area.

Figure 3 | Space/spectrum cross correlation (SSCC) of a lasing random cavity. **a** CCD image of spatially and spectrally resolved intensity profile plotted as 'slit height', h in μm vs. λ. **b** The intensity profile of the main laser mode at ~630.8 nm computed from the SSCC image in **a**. **c** The emission spectrum obtained by integrating the CCD image from **a** over its h-columns for each wavelength. **d** PFT of the emission spectrum shown in **c**.

Figure 4 | Detailed **space/spectrum cross correlation (DSSCC) spectroscopy of two competing cavities in the excited area. a** False color image of the total intensity in each of the 400 10x10 μm^2 spot of the excited film area. The two squares symbolize two 'lasing random cavities' in the film, where each contains a 9-pixel cluster. **b** The sum of the emission spectra of the two '9-pixel clusters' in **a**; where the left (right) spectrum corresponds to the left (right) 'cavity' in **a**. **c** Same as in **b** but for the average PFT of the 9-pixel clusters, where we add the PFT of the RL emission spectrum in each pixel belonging to the cluster. Note the main Fourier component at d ~ 45 (50) micron for the left (right) 'cavity'; and their harmonics.

Figure 5 | a The DSSCC of the excited area, as in Fig. 4a, for better comparison with b. **b** The summed RL emission spectrum in the **h**-pixels at each translation position, X_i, denoted on the y-axis. Note that the y-axis in **b** corresponds to the **x** direction in **a**. It is noteworthy that apart from X_i = H, each laser mode is localized within its respective 'half' that corresponds to the left or right cavities in **a**.

Figure 6 | Random lasing intensity threshold histograms, $F^{(n)}(I_{th})$. a The first three I_{th} distribution functions, $F^{(n)}(I_{th})$ of RL in a pristine DOO-PPV polymer film at a fixed excitation area of 100 μm x 1 mm. $F^{(1)}(I_{th})$ is for the cavity with the highest Q-value within the excited area, and thus lowest I_{th}. $F^{(2)}(I_{th})$ and $F^{(3)}(I_{th})$ are for RL cavities with second and third highest Q-values in the excited film area, and thus have higher I_{th}. **b** $F^{(1)}(I_{th})$ in a DOO-PPV film at three different excitation areas, S as noted. The lines through the histograms is a model fit using Eq. (3) with parameters given in Table I.

Figure 7 | Random lasing in DOO-PPV films mixed with TiO_2 nanoparticles at various concentrations, ρ. a Coherent backscattering (CBS) cone from thick films of DOO-PPV mixed

with TiO_2 nanoparticles, plotted at various ρ. **b** The light mean free path, ℓ_s as extracted from the fit to the CBS cones shown in **a**; the line through the data is to 'guide the eye'. **c** $F^{(1)}(I_{th})$ at a fixed excitation area of 100 μm x 1 mm for various **ρ** as shown. The lines through the histograms is a model fit based on Eq. (3) with parameters given in Table I. **d** Average I_{th}, $(I_{th})_{ave}$ versus ρ, as obtained from the $F^{(1)}(I_{th})$ in **c**.

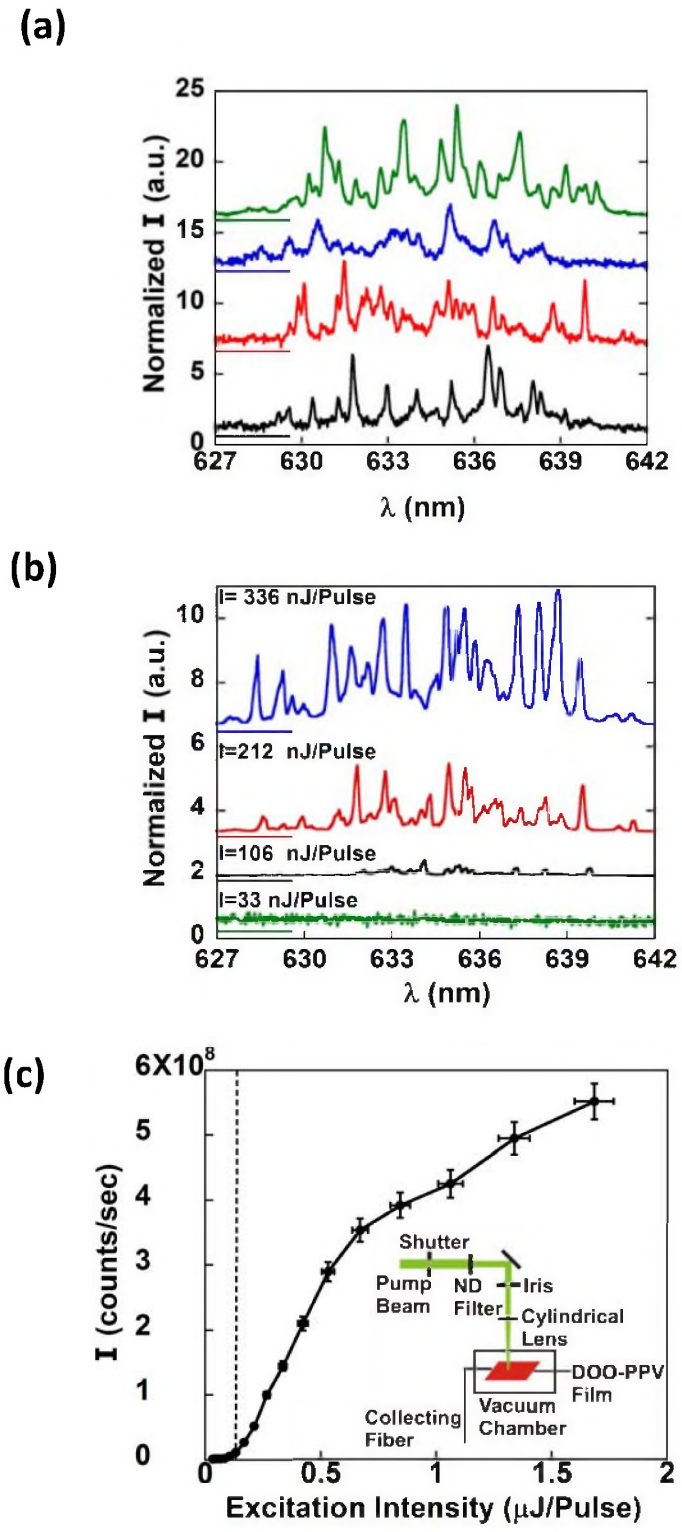

FIGURE 1

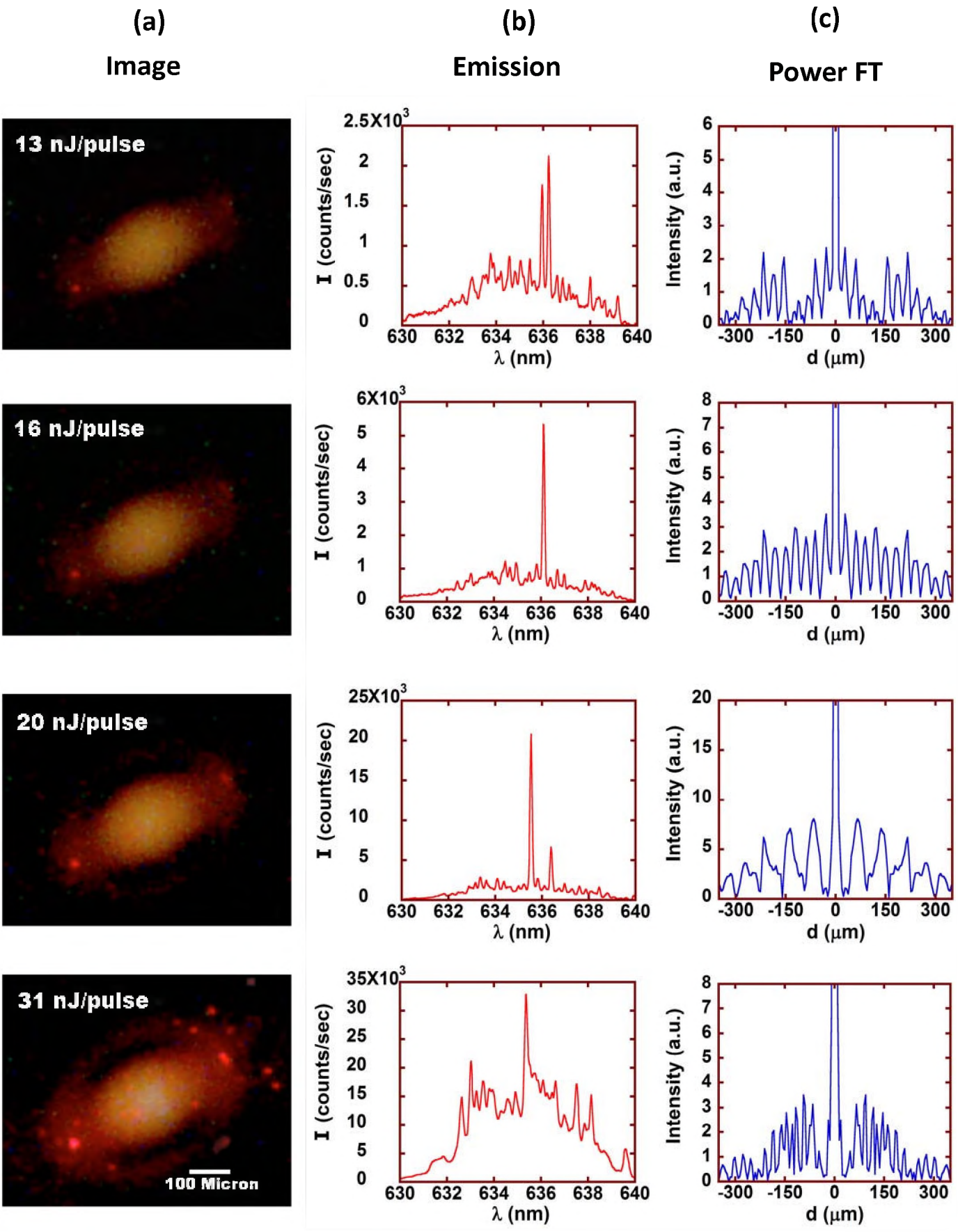
(a)
Image
(b)
Emission
(c)
Power FT
13 nJ/pulse
16 nJ/pulse
20 nJ/pulse
31 nJ/pulse
100 Micron
I (counts/sec)
λ (nm)
Intensity (a.u.)
d (μm)
2.5X10^3
6X10^3
25X10^3
35X10^3

FIGURE 2

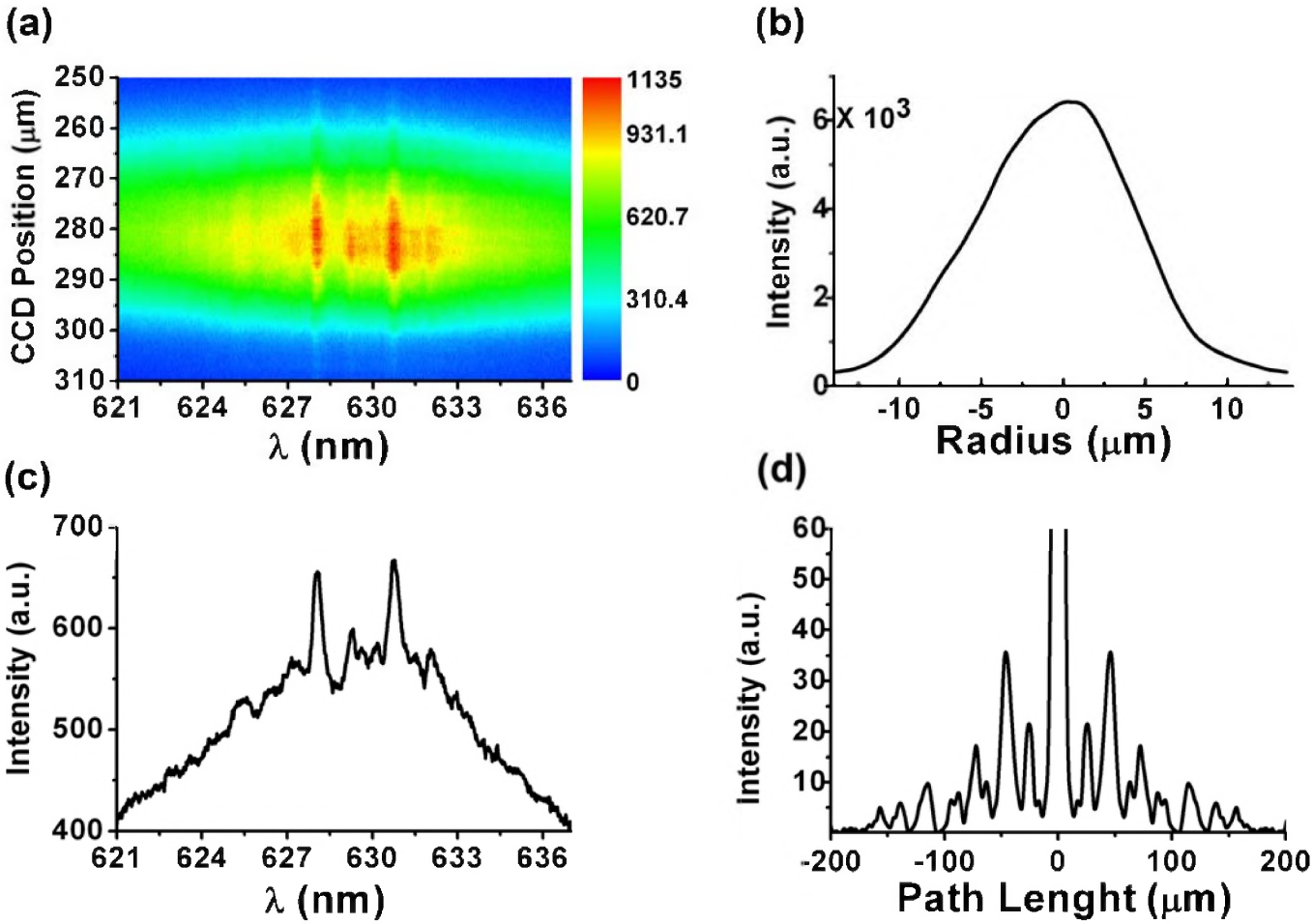

FIGURE 3

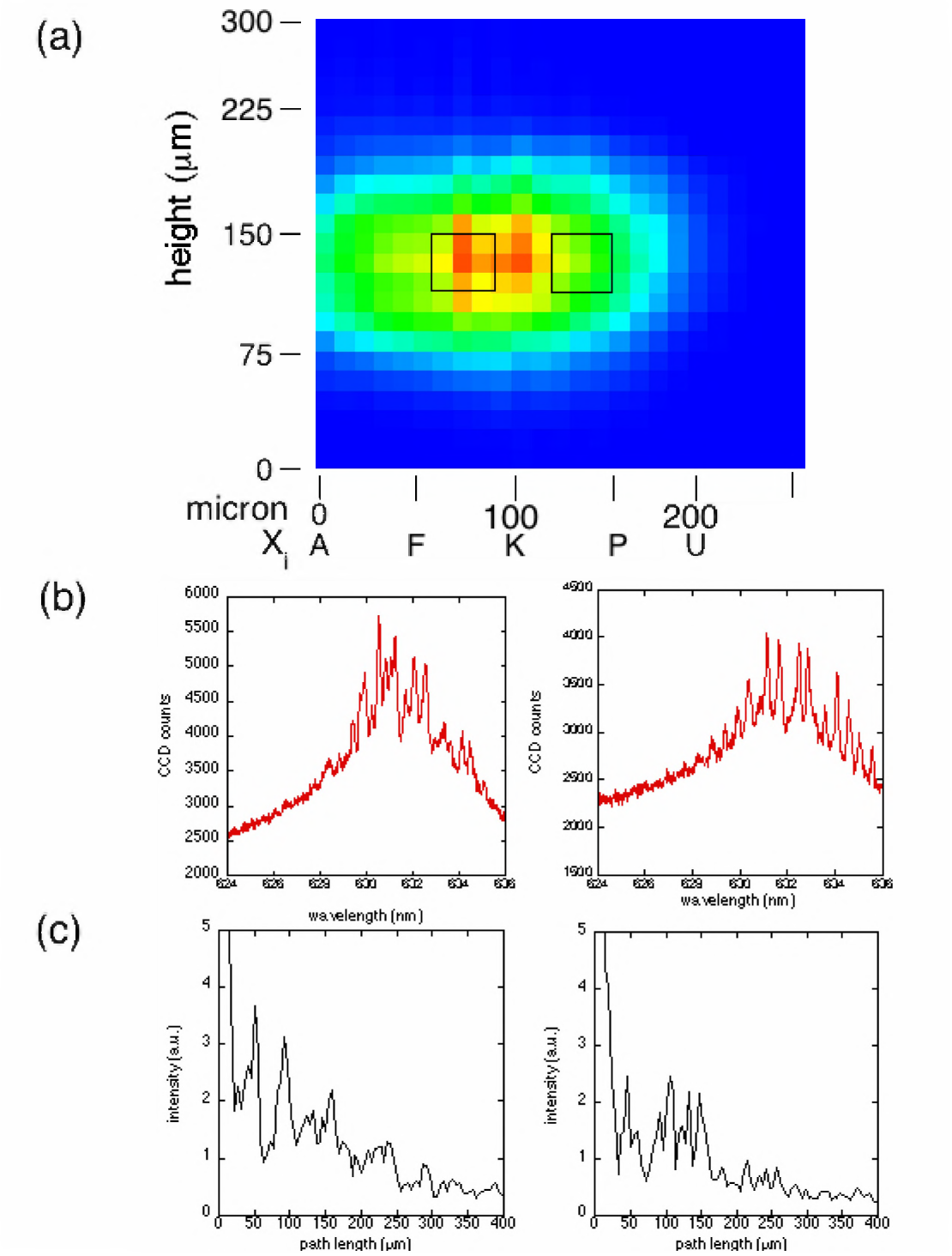

FIGURE 4

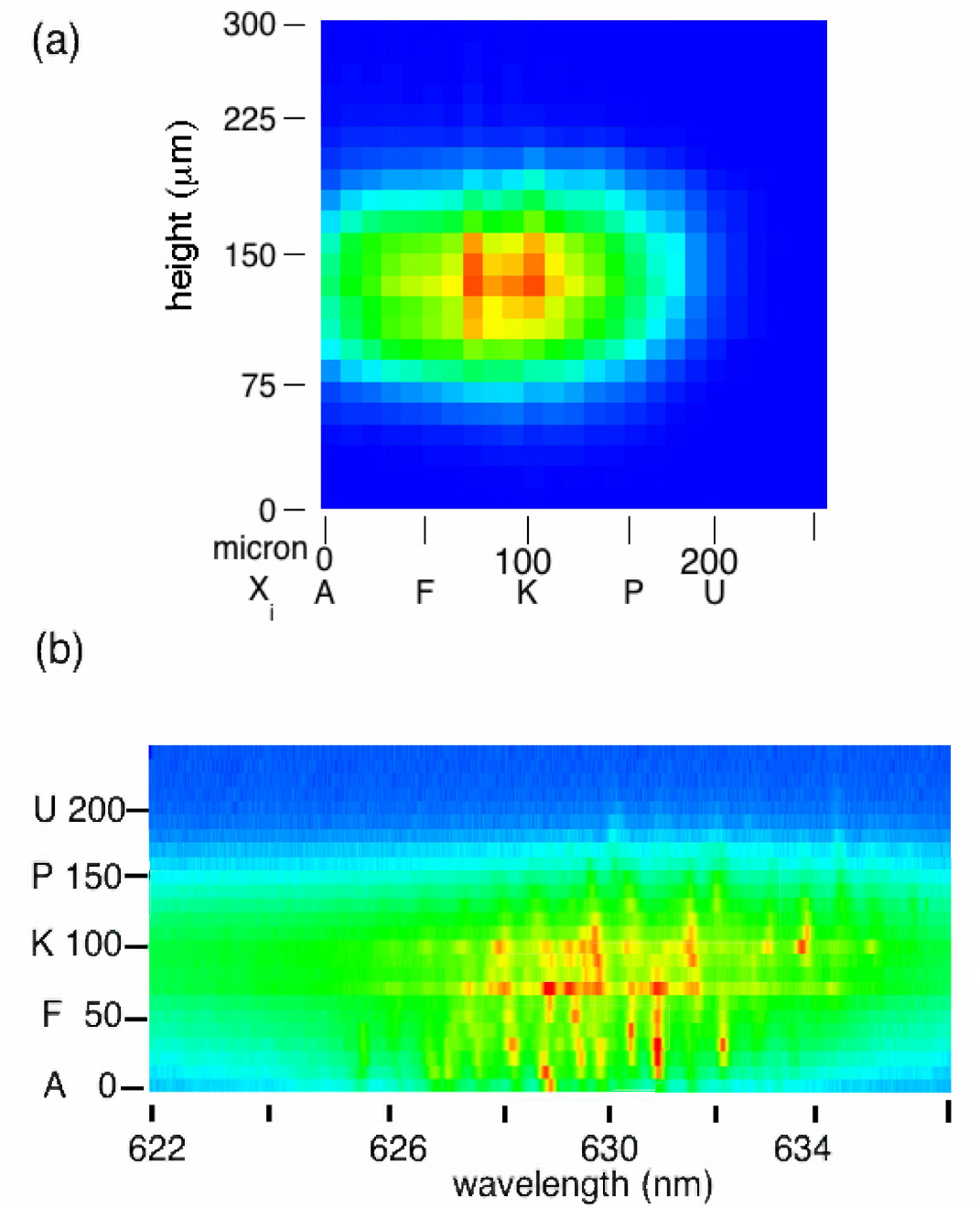

FIGURE 5

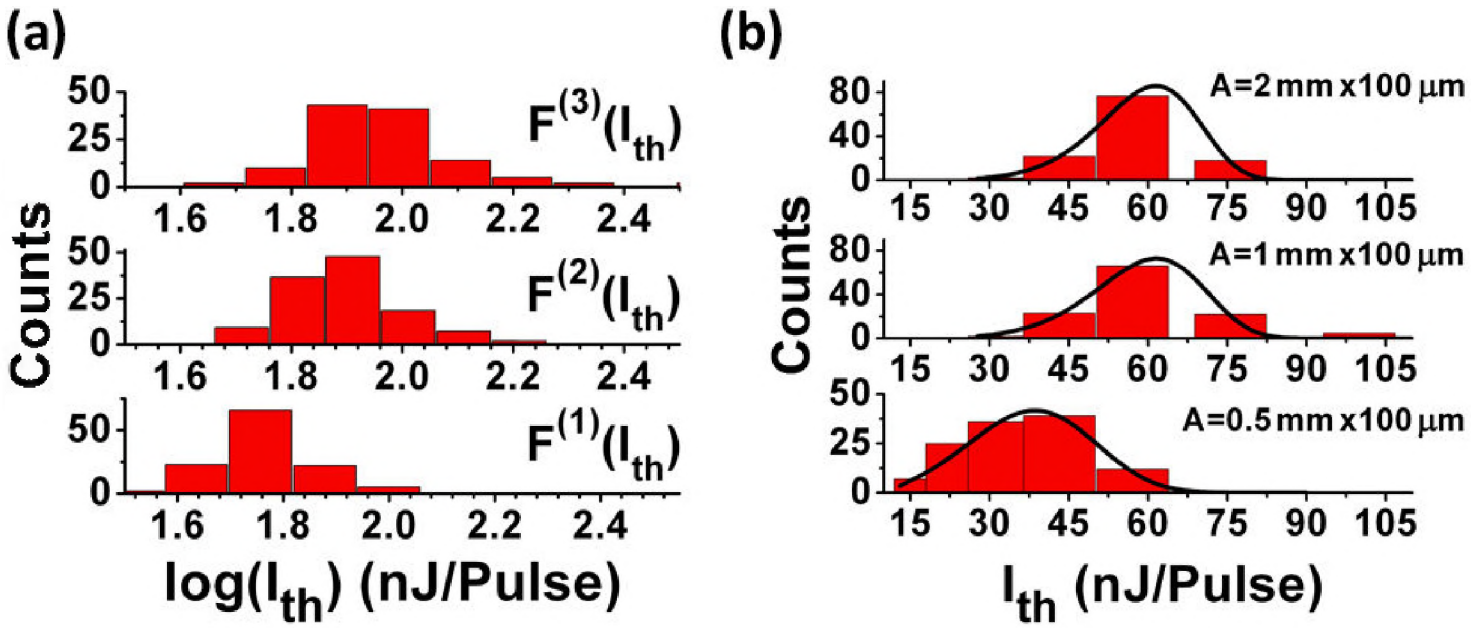
(a)
(b)
Counts
$F^{(3)}(I_{th})$
$F^{(2)}(I_{th})$
$F^{(1)}(I_{th})$
$\log(I_{th})$ (nJ/Pulse)
A=2 mm x100 μm
A=1 mm x100 μm
A=0.5 mm x100 μm
I_{th} (nJ/Pulse)

FIGURE 6

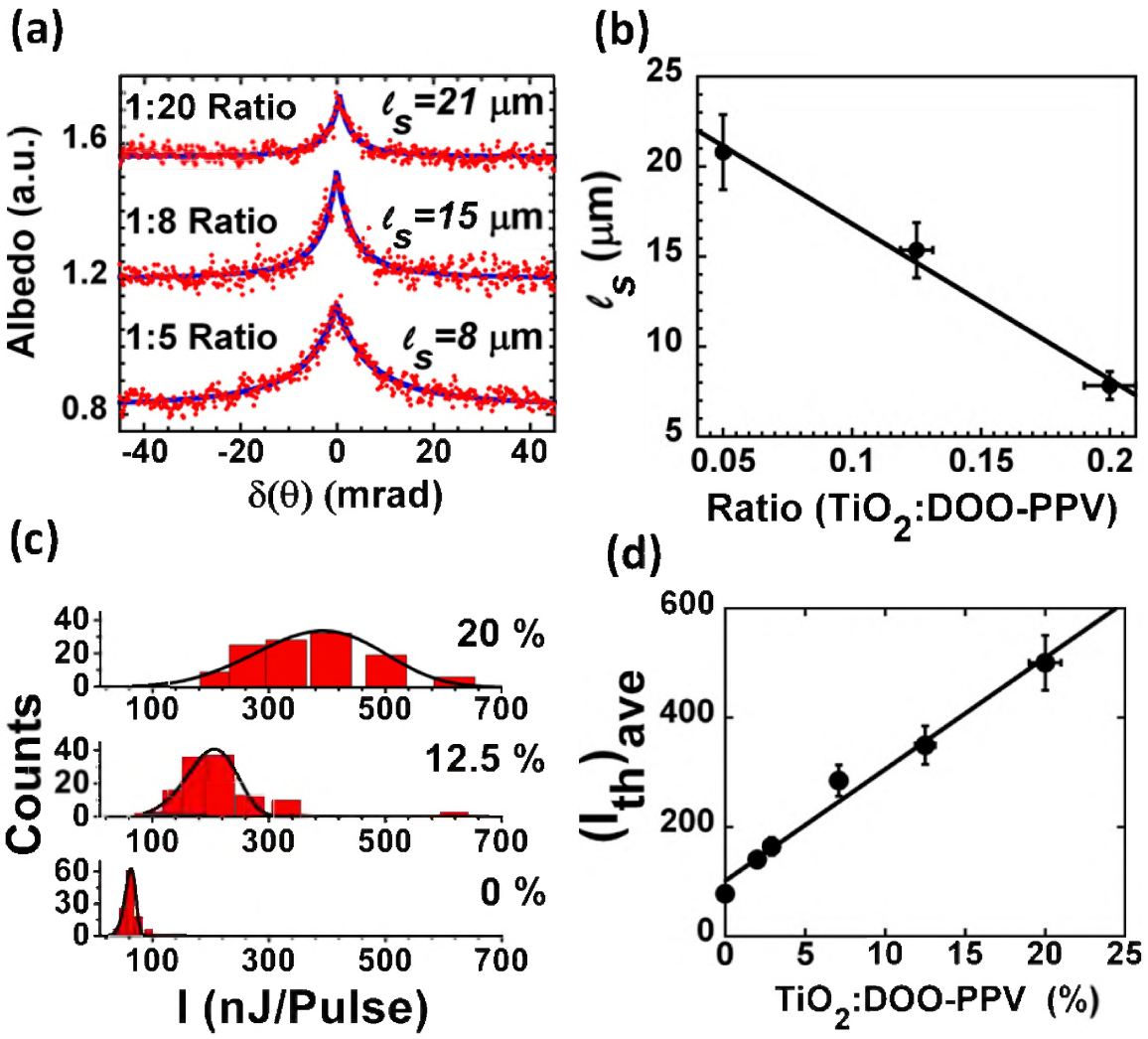

FIGURE 7